vations of a discontinuity near 1150 km in subduction areas [(3, 6), for example] indicates that this may be a global feature of yet unknown nature.

The observation of reflectors at midmantle depths comparable to those in subduction zones, but in a different environment, indicates that a search for yet unidentified mineral assemblages of global significance may be worthwhile. Recent experiments have shown the possible existence of phase transitions at lower mantle conditions: orthorhombic-to-cubic silicate perovskite (*30*) and rutile SiO_2 to $CaCl_2$ structure (*31*). The role and proportions of volatiles such as water or carbon dioxide in the mantle remain largely unknown and could be of importance (*32*).

Additional seismic observations with the great resolving power of BB arrays should help answer the question of the global character of our observations.

REFERENCES AND NOTES

1. L. R. Johnson, *Bull. Seismol. Soc. Am.* **59**, 973 (1969).
2. J. H. Whitcomb and D. L. Anderson, *J. Geophys. Res.* **75**, 5713 (1970).
3. L. P. Vinnik, A. A. Lukk, A. V. Nikolaev, *Phys. Earth Planet. Inter.* **5**, 328 (1972).
4. H. Kawakatsu and F. Niu, *Nature* **371**, 301 (1994).
5. N. Petersen, J. Gossler, R. Kind, K. Stammler, L. Vinnik, *Geophys. Res. Lett.* **20**, 281 (1993).
6. C. W. Wicks and M. A. Richards, *Eos Fall Suppl.* **74**, 550 (1993).
7. E. R. Engdahl and E. A. Flinn, *Science* **163**, 177 (1969).
8. R. D. Adams, *Bull. Seismol. Soc. Am.* **61**, 1441 (1971).
9. I. Nakanishi, *Geophys. Res. Lett.* **13**, 1458 (1986).
10. ———, *Geophys. J. Int.* **93**, 335 (1988).
11. J. P. Davis, R. Kind, I. S. Sacks, *ibid.* **99**, 595 (1989).
12. P. G. Richards, *Z. Geophys.* **38**, 517 (1972).
13. H. M. Benz and J. E. Vidale, *Nature* **365**, 147 (1993).
14. L. P. Vinnik, R. A. Avetisjan, N. G. Mikhailova, *Phys. Earth Planet. Int.* **33**, 149 (1983).
15. N. Petersen *et al.*, *Geophys. Res. Lett.* **20**, 859 (1993).
16. V. S. Solomatov and D. J. Stevenson, *Earth Planet. Sci. Lett.* **125**, 267 (1994).
17. B. L. N. Kennett and E. R. Engdahl, *Geophys. J. Int.* **105**, 429 (1991).
18. C. H. Scholz, T. A. Koczynski, D. G. Hutchins, *Geophys. J. R. Astron. Soc.* **44**, 135 (1976).
19. G. S. Wagner and C. A. Langston, *Geophys. J. Int.* **94**, 503 (1988).
20. D. S. Chapman and H. N. Pollack, *Tectonophysics* **41**, 79 (1977).
21. S. P. Grand, *IUGG Abstr. Week B* **74**, 395 (1995).
22. P. M. Shearer and T. G. Masters, *Nature* **355**, 791 (1992).
23. E. Ito and E. Takahashi, *J. Geophys. Res.* **94**, 10637 (1989).
24. R. A. W. Haddon, E. S. Husebye, D. W. King, *Phys. Earth Planet. Int.* **14**, 41 (1977).
25. A. M. Dziewonski, A. M. Forte, W.-J. Su, R. L. Woodward, *AGU Geophys. Monogr.* **76**, 67 (1993).
26. W.-J. Su, R. Woodward, A. M. Dziewonski, *J. Geophys. Res.* **99**, 6945 (1994).
27. T. G. Masters, H. Bolton, P. Shearer, *EOS Spring Suppl.* **73**, 201 (1992).
28. X. D. Li and B. Romanowicz, *Geophys. J. Int.* **121**, 695 (1995).
29. Bukowinski and Wolf (*33*) calculate that changes in symmetry of silicate perovskite would involve a positive Clapeyron slope. If the 900-km discontinuity has a negative slope as we suggest, this would rule out a structural change in perovskite as a cause of the 900-km discontinuity, in agreement with (*34*).
30. C. Meade, H. K. Mao, J. Hu, *Science* **268**, 1743 (1995).
31. K. J. Kingma, R. E. Cohen, R. J. Hemley, H.-K. Mao, *Nature* **374**, 243 (1995).
32. J. A. Tyburczy, T. S. Duffy, T. J. Ahrens, M. A. Lange, *J. Geophys. Res.* **96**, 18011 (1991).
33. M. S. T. Bukowinski and G. H. Wolf, *ibid.* **95**, 12583 (1990).
34. L. Stixrude and R. E Cohen, *Nature* **364**, 613 (1993).
35. K. J. Muirhead and R. Datt, *Geophys. J. R. Astron. Soc.* **47**, 197 (1976).
36. This amplitude difference comes from the fact that there is less coherence in the SP data than in BB data, so that using a large number of stations attenuates small signals, whereas larger signals are unaffected. This is, however, concomitant to a reduction in noise amplitude (*35*) so that coherent phases can be detected.
37. We thank L. Vinnik for comments and suggestions and J. Vidale for providing short-period array data. This study was partially supported by the France-Berkeley Fund and is the Berkeley Seismographic Station contribution 95-6.

1 May 1995; accepted 1 August 1995

Coherent Laser Control of the Product Distribution Obtained in the Photoexcitation of HI

Langchi Zhu, Valeria Kleiman, Xiaonong Li, Shao Ping Lu,*
Karen Trentelman,† Robert J. Gordon‡

Active control of the distribution of products of a chemical reaction was demonstrated by using a method based on the principle of quantum mechanical interference. Hydrogen iodide (HI) molecules were simultaneously excited above their ionization threshold by two competing pathways. These paths were absorption of three ultraviolet photons of frequency ω_1 and one vacuum ultraviolet photon of frequency $\omega_3 = 3\omega_1$. The HI^+ and I^+ signals were modulated as the phase between the lasers was varied, with the HI^+ signal lagging by 150° ± 15°. A mechanism consisting of autoionization and predissociation is proposed.

A fundamental goal in synthetic chemistry is to develop methods for maximizing the yield of a desired compound while reducing the yields of unwanted by-products. The traditional approach to this problem is to modify the experimental conditions (such as temperature, pressure, or pH) so as to optimize the product distribution. This is a passive strategy in that it relies on the natural response of the chemical system to external conditions, and there is no guarantee that there exist conditions that could produce the desired result. For example, one may wish to photodissociate the stronger of two bonds in a molecule. Although for some molecules it may be possible to find wavelengths of light that can accomplish this task (*1*), for many others the weakest bond breaks preferentially at any wavelength.

In recent years, a number of strategies have been proposed to achieve more active control of chemical reactions (*2*). The central idea is to manipulate the reacting molecule with electromagnetic fields, which allow the experimenter to guide the molecule along the desired reaction path. We report here active experimental control of the distribution of products in a chemical reaction.

One approach for controlling chemical reactions, developed by Tannor, Rice, and co-workers (*3*), is to excite a molecule with a sequence of ultrashort light pulses. This method has been used, for example, by Gerber and co-workers (*4*) to control the ionization and fragmentation of Na_2.

Another approach to active control is based on the principle of quantum-mechanical interference. This principle states that if there exist more than one independent way of reaching a final state, the overall probability of reaching that state includes the probabilities of the individual paths and contributions arising from interference between them. The best known example of this principle is the interference of particles passing through a pair of slits before hitting a screen. The intensity of particles reaching some point on the screen is the sum of the intensities obtained from each slit independently, plus an interference term that depends on the relative distance of the point from the two slits.

The photochemical analog of the two slit experiment was first proposed by Brumer and Shapiro (*3*). Their strategy involves the simultaneous excitation of a molecule by two different pathways connecting the same initial and final states. The probability for each independent transition is given by:

$$P_n \propto |\langle \Psi_f | \hat{O}_n | \Psi_i \rangle|^2 \qquad (1)$$

where ψ_i and ψ_f are the time-independent

Department of Chemistry (m/c 111), University of Illinois at Chicago, Chicago, IL 60607-7061, USA.

*Present address: Department of Chemistry, Indiana University, Bloomington, IN 47405, USA.

†Present address: Detroit Institute of Arts, 5200 Woodward Avenue, Detroit, MI 48202, USA.

‡To whom correspondence should be addressed.

wave functions describing the initial and final states and $\hat{O}_n$ is the transition operator for pathway n. When both pathways are present, the combined probability is:

$$P_{\mathrm{tot}} = P_1 + P_2 + P_{12} \cos\Delta\phi \qquad (2)$$

where $P_{12} \cos\Delta\phi$ results from interference between the paths and $\Delta\phi$ is a phase difference associated with the two paths. The total reaction probability can be modulated by varying $\Delta\phi$ experimentally.

In our experiment, the two optical pathways are excitation with three photons of frequency ω_1 or with a single photon of frequency $\omega_3 = 3\omega_1$ (4). In this case the phase difference is given by:

$$\Delta\phi = \phi_3 - 3\phi_1 + \delta_{13} \qquad (3)$$

Here ϕ_3 and ϕ_1 are constant terms in the phases of the two electromagnetic fields, and δ_{13} is a "molecular phase" derived from the complex value of ψ_f. Variation of the "laser phase" ϕ_3-$3\phi_1$ allows control of the population of the final state.

This concept can be taken a step further to control the ratio of products evolving from the excited molecule. In this case, the excited state wave function can be written as a superposition of two outgoing waves, each correlating asymptotically to a different set of products. The coefficients of this superposition depend on the phases of the two fields and of the outgoing wave, so that the probability of obtaining a particular product q may be controlled by changing the laser phase. For the one- and three-photon paths, this probability is given by (5):

$$P^q \propto I_3 S_3^q + I_1^3 S_1^q$$
$$+ \; 2[I_3 I_1^3]^{1/2} S_{13}^q \cos(\phi_3 - 3\phi_1 + \delta_{13}^q) \qquad (4)$$

In this expression, $I_3 S_3^q$ is the probability of obtaining product q after absorption of one photon, $I_1^3 S_1^q$ is the three-photon probability, and the last term is caused by quantum-mechanical interference (I_j is the intensity of light at frequency ω_j, S_j^q are absorption coefficients, and S_{13}^q is a matrix element of the product of the one- and three-photon operators). Selective control of a particular product is possible if the molecular phases δ_{13}^q for various reaction channels differ sufficiently.

Calculations have demonstrated the feasibility of this approach (5, 6), but experimental progress has been slow. Coherent phase control of a bound-to-bound transition (in which the only product is a bound excited state, and $\delta_{13}^q = 0$) was first demonstrated for atoms by Bucksbaum and co-workers (7) and later by Elliott and co-workers (8), whereas control of diatomic molecules was achieved by Gordon and co-workers (9, 10). Elliott and co-workers (11) have also demonstrated that the direction of electrons released in photoionization of atoms and diatomic molecules may be controlled coherently.

For bound-to-continuum transitions of molecules, it was necessary to show that averaging P^q over rotational states does not wash out the interference. Another concern was that three-photon–allowed, one-photon–forbidden transitions might mask the modulation. Our recent control of the direct ionization of H_2S (12) demonstrates that these are not major obstacles for control. In all of these experiments, control was observed for only a single set of products.

We show in this report that quantum-mechanical interference can be used to control the branching ratio in a chemical reaction. By varying the phase difference between two laser beams, we controlled the relative amounts of HI^+ and I^+ produced in the photoexcitation of HI. In this experiment, a vacuum ultraviolet (VUV) photon at 118.33 nm and three UV photons at 354.98 nm were used to excite HI above its ionization threshold. The UV photons were produced with an excimer-pumped dye laser (Lambda Physik Lextra 50 and Scanmate II, DMQ dye, ~2.0 mJ per pulse at 10 Hz). The VUV radiation was produced from the UV beam by third-harmonic generation (THG) in a cell containing 2 to 3 torr of Xe. The Xe pressure was adjusted so that the total product yields from the two paths were approximately equal. The conditions of THG guarantee that the laser phase ϕ_3-$3\phi_1$ is a constant after emerging from the tripling cell (13). In order to maximize the yield of a particular product, it is necessary to vary ϕ_3-$3\phi_1$, which was accomplished by passing both beams through a tuning cell containing H_2 gas. By exploiting the difference between the refractive indices of

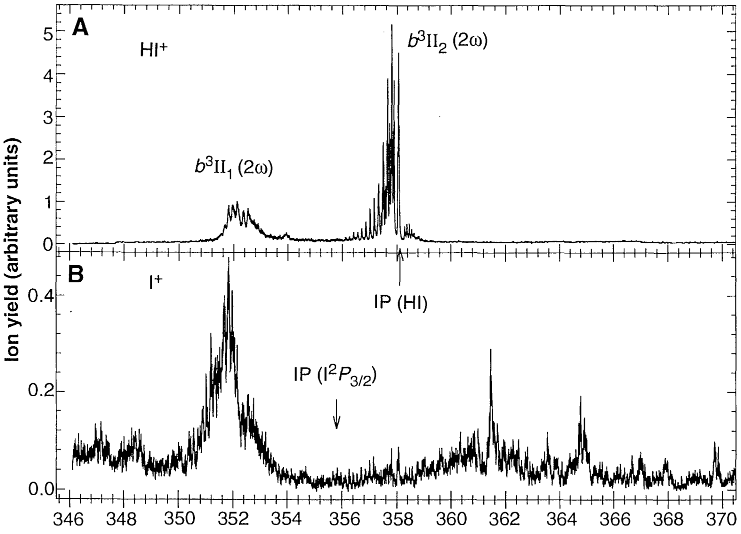

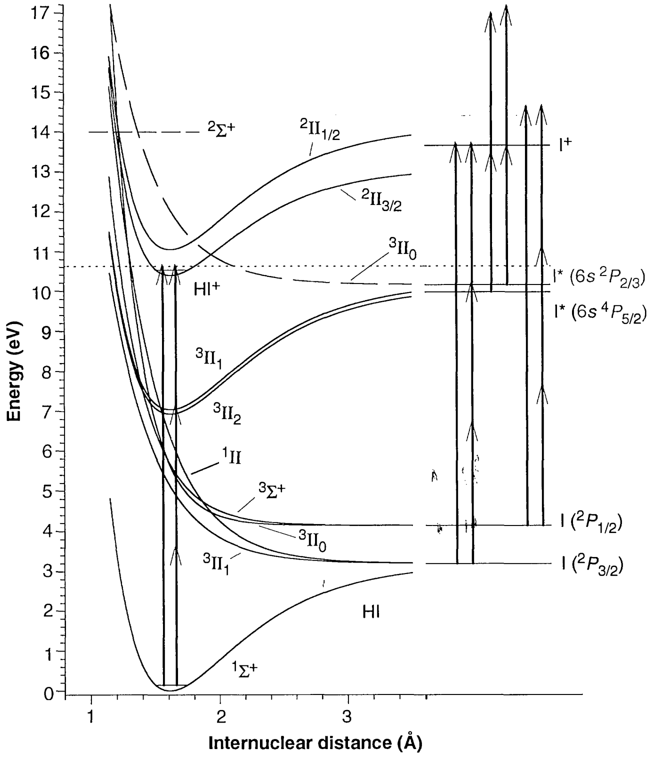

Fig. 1 (**left**). The UV photoionization spectrum of HI. (**A**) The HI^+ signal, including two-photon resonance-enhanced ionization from two of the $b\,^3\Pi_i$ Rydberg states. (**B**) The I^+ signal, with strong enhancement of the ion yield in the vicinity of the $b\,^3\Pi_1$ HI resonance. The ionization thresholds of HI and $I(^2P_{3/2})$ by three UV photons are indicated with arrows. **Fig. 2** (**right**). Potential energy diagram for HI and I, obtained from (15–18). The short and long arrows on the left indicate the mechanism for controlling the excitation of HI. The arrows on the right indicate possible schemes for ionizing the iodine fragment. The horizontal dotted line corresponds to the energy of three 354.98-nm photons at which one of the phase-control experiments was performed.

H_2 in the UV and VUV, a phase lag between the two beams is produced. This relative phase difference can be altered by simply changing the pressure in the tuning cell (*14*). The two beams were focused with a pair of Al/MgF_2-coated mirrors (20.3-cm focal length) into an unskimmed pulsed molecular jet of HI, and the product ions were detected with a time-of-flight mass spectrometer. Additional experimental details have been reported previously (*10*).

Figure 1 shows the three-photon photoionization spectrum obtained with the UV beam. The rotational structure in the HI^+ signal results from 2+1 resonance-enhanced multiphoton ionization (REMPI) of the $b^3\Pi_2$ and $b^3\Pi_1$ Rydberg states (*15*). The $b^3\Pi_1$ state is strongly predissociated and produces I atoms that are responsible for the peak seen in the I^+ spectrum near 351.8 nm. Potential energy curves (*15–18*) and energy levels for the states involved are shown in Fig. 2.

In order to avoid complications arising from intermediate resonances, the experiment was performed at wavelengths lying between the REMPI features shown in Fig. 1. Coherent control of the HI^+ and I^+ signals at 354.98 nm (3.49 eV) is shown in Fig. 3. As the phase difference between the UV and VUV beams was varied, both ion signals oscillated. The modulation frequencies for the two ions are within 1% of each other and agree with the value predicted from the refractive indices of hydrogen (*14, 18*). Although the yield for HI^+ is approximately three times greater than that for I^+, their modulation depths are nearly the same. Moreover, they are comparable to the modulation obtained for bound-to-bound transitions under similar experimental conditions (*14, 18*). The key point is that the HI^+ and I^+ signals are out of phase, so that when one signal is at a maximum the other is near a minimum.

The lag between the signals was determined quantitatively from their correlation coefficient. We first corrected the scans for a slow linear baseline drift and then rescaled the signals so that their average values were zero and their intensities were equal. The correlation coefficient ρ_s is defined as:

$$\rho_s = \frac{1}{N} \sum_{i=1}^{N} X_i Y_{i+s} \tag{5}$$

where X_i is the HI^+ signal at hydrogen pressure i, Y_{i+s} is the I^+ signal at pressure $i+s$, and N is the number of points in the scan. The offset s was varied so as to maximize ρ_s. Twenty scans, taken over a period of several weeks, gave a lag of 150° ± 15° (1 σ). Our observation of a lag between the two ion signals is in contrast to our finding for H_2S, where the signals for H_2S^+, HS^+, and S^+ were all in phase (*12*). In that case, we demonstrated that HS^+ and S^+ were produced by photodissociation of the parent ion, and only the total ion yield was controlled. Here, the lag between HI^+ and I^+ clearly rules out this mechanism.

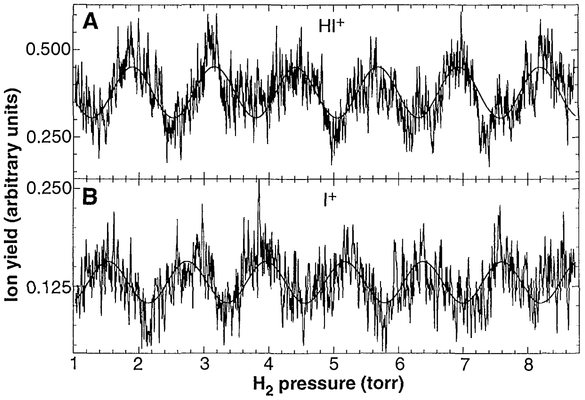

Fig. 3. Modulation of the (**A**) HI^+ and (**B**) I^+ signals as functions of H_2 pressure in the phase-tuning cell. The HI^+ signal is seen to lag the I^+ signal by ~150°. The smooth curves are least-squares fits of the function $A + B\cos(cP+d)$. The frequency c agrees with the value calculated from the refractive index of H_2 at ω_1 and ω_3.

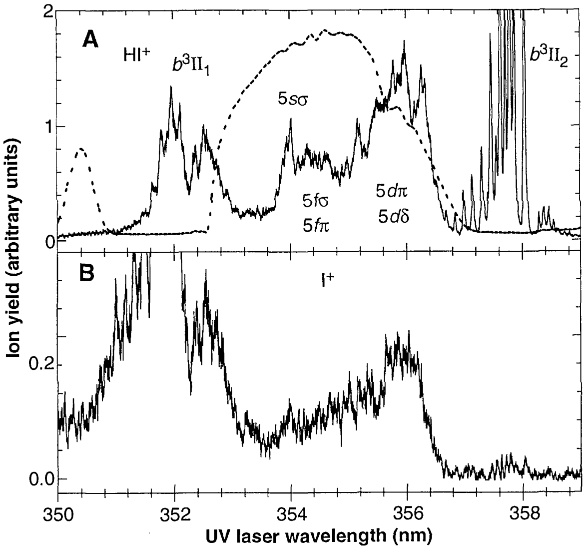

Fig. 4. Photoionization spectrum of HI obtained by adding 12 torr of Xe to the frequency-tripling cell. This spectrum is the sum of both the UV- and VUV-generated signals. The autoionization structure of HI between 353.8 and 356.2 nm is visible in both the (**A**) HI^+ and (**B**) I^+ data. The dashed line shows the THG efficiency in Xe.

The most plausible explanation of our data is that a superexcited state of HI undergoes both autoionization and predissociation:

$$HI + (\omega_3, 3\omega_1) \rightarrow HI + e^- \tag{6}$$

$$HI + (\omega_3, 3\omega_1) \rightarrow H + I \tag{7}$$

and that the branching between these two reactions is controlled by varying the phase difference between the two laser beams. Control of the autoionization of Xe, which is isoelectronic with HI, was predicted by Nakajima and Lambropoulos (6). Our proposed mechanism is a generalization of this problem to the case of a superexcited state embedded in two continua.

As shown in Fig. 2, the energetically possible states of the iodine atom are $5p^5$ ($^2P_{3/2}$), $5p^5$ ($^2P_{1/2}$), $6s$ ($^4P_{5/2}$), and $6s$ ($^2P_{3/2}$). Depending on which states are populated, the I atoms formed in reaction 7 absorb two or three UV photons to produce I^+ ions. The lag between the two ion signals in Fig. 3 is due to the difference between the molecular phases for reactions 6 and 7.

An alternate mechanism that must be considered is the dissociation of HI at the two photon level (at the long wavelength edge of the 351.8-nm peak in Fig. 1B) to produce $I(^2P_{3/2})$, followed by an additional pair of controlling steps:

$$HI + 2\omega_1 \rightarrow H + I(^2P_{3/2}) \tag{8}$$

$$I(^2P_{3/2}) + (\omega_3, 3\omega_1) \rightarrow I^+ + e^- \tag{9}$$

Previous work (*16, 19*) showed that only a few percent $I(^2P_{1/2})$ is formed at this energy. If this mechanism were correct, the lag between the two ion signals would be due to the difference between the molecular phases for reactions 6 and 9.

One way of distinguishing between these mechanisms is to compare the one- and three-photon spectra of HI^+ and I^+. To do this, we increased the intensity of VUV radiation by increasing the pressure of Xe in the tripling cell. As shown in Fig. 4, between 353.8 and 356.25 nm (117.93 to 118.73 nm in the VUV) both ion signals are dominated by autoionization resonances of HI, indicating that

I atoms are produced at the $\omega_3 = 3\omega_1$ energy level (at ~10.6 eV). This signature is also evident in the modulation data. Between 354.98 and 356.18 nm, which corresponds to the region of the $5d\pi$ and $5d\delta$ resonances of HI (*20*), we obtained control with a 150° lag between the two signals. Between 354.28 and 354.88 nm (the region of the $5f\sigma$ and $5f\pi$ resonances), we saw little or no modulation of the ion signals, while between 353.78 and 354.23 nm (the region of the $5s\sigma$ resonance) we again obtained modulation, but in this case there was no lag between the HI^+ and I^+ signals. Finally, for wavelengths shorter than 353.78 nm, modulation was again absent.

In order to obtain phase modulation of I^+, the controlled state must be reached by both ω_3 and $3\omega_1$. Because HI autoionization structure dominates the ω_3 spectrum of I^+ (Fig. 4B), it follows that I atoms are produced by ω_3 and $3\omega_1$ at 10.6 eV (*21*). This evidence rules out the second mechanism, which produces I at the $2\omega_1$ level. Moreover, the autoionizing structure of $I(^2P_{3/2})$ is absent in the I^+ spectrum (Fig. 1B). In particular, a strong resonance at the atomic ionization threshold (*22*) is conspicuously absent in this spectrum. Also, tuning the UV laser to the 2+1 REMPI frequencies of $I(^2P_{1/2,\ 3/2})$ failed to produce any structure in the I^+ spectrum (Fig. 1B). If two photons produce an excess of I atoms, both of these features would be prominent in the spectrum.

Another possibility involving two sequential control steps (for example, reactions 7 and 9) can be also ruled out, because this mechanism would cause I^+ to have twice the modulation frequency of HI^+.

We have controlled the outcome of a chemical reaction by quantum-mechanical interference between competing excitation paths. We have used two laser beams to promote the HI molecule to a state that is embedded in both autoionization and predissociation continua. By varying the phase difference between the two beams we favor one reaction product over the other. The ultimate goal of using lasers to break specific bonds in a molecule appears to be within reach.

REFERENCES AND NOTES

1. E. Jensen *et al.*, *J. Chem. Phys.* **98**, 1882 (1993).
2. W. S. Warren, H. Rabitz, M. Dahleh, *Science* **259**, 1581 (1993); S. A. Rice, *ibid.* **258**, 412 (1992).
3. R. Kosloff, S. A. Rice, P. Gaspard, S. Tersigni, D. J. Tannor, *Chem. Phys.* **139**, 201 (1989).
4. T. Baumert, M. Grosser, R. Thalweiser, G. Gerber, *Rev. Phys. Lett.* **67**, 3753 (1991).
5. C. K. Chan *et al.*, *J. Chem. Phys.* **94**, 2688 (1991); A. D. Bandrauk, J. Gauthier, F. J. McCann, *ibid.* **100**, 340 (1994); M. Shapiro and P. Brumer, *ibid.* **84**, 4103 (1986); T. Nakajima, P. Lambropoulos, S. Cavalieri, M. Matera, *Phys. Rev. A* **46**, 7315 (1992).
6. T. Nakajima and P. Lambropoulos, *Phys. Rev. Lett.* **70**, 1081 (1993); *Phys. Rev. A* **50**, 595 (1994).
7. H. G. Muller, P. H. Bucksbaum, D. W. Schumacher, A. Zavriyev, *J. Phys. B* **23**, 2761 (1990).
8. C. Chen, Y.-Y. Yin, D. S. Elliott, *Phys. Rev. Lett.* **64**, 507 (1990); C. Chen and D. S. Elliott, *ibid.* **65**, 1737 (1990).
9. S. M. Park, S.-P. Lu, R. J. Gordon, *J. Chem. Phys.* **94**, 8622 (1991).
10. S. Lu, S. M. Park, Y. Xie, R. J. Gordon, *ibid.* **96**, 6613 (1992).
11. Y.-Y. Yin, C. Chen, D. S. Elliott, *Phys. Rev. Lett.* **69**, 2353 (1992); Y.-Y. Yin, D. S. Elliott, R. Shehadeh, E. R. Grant, *Chem. Phys. Lett.* **241**, 591 (1995).
12. V. Kleiman, L. Zhu, X. Li, R. J. Gordon, *J. Chem. Phys.* **102**, 5863 (1995).
13. M. Bjorklund, *IEEE J. Quant. Electron.* **QE-11**, 287 (1975).
14. R. J. Gordon *et al.*, *J. Chem. Phys.* **98**, 9481 (1993).
15. S. G. Tilford, M. L. Ginter, A. N. Bass, *J. Mol. Spectrosc.* **34**, 327 (1970).
16. G. N. A. Van Veen, K. A. Mohamed, T. Baller, A. E. de Vries, *Chem. Phys.* **80**, 113 (1983).
17. K. Huber and G. Herzberg, *Molecular Spectra and Molecular Structure* (Van Nostrand Reinhold, New York, 1979), vol. 4; N. Böwering, H. Klausing, M. Müller, M. Salzmann, U. Heinzmann, *Chem. Phys. Lett.* **189**, 467 (1992); S. Pratt, *J. Chem. Phys.* **101**, 8302 (1994).
18. C. J. Zietkiewicz, Y.-Y. Gu, A. M. Farkas, J. G. Eden, *J. Chem. Phys.* **101**, 86 (1994).
19. I. Levy and M. Shapiro, *ibid.* **89**, 2900 (1988).
20. J. H. D. Eland and J. Berkowitz, *ibid.* **67**, 5034 (1977); D. J. Hart and J. W. Hepburn, *Chem. Phys.* **129**, 51 (1989).
21. From Fig. 4, we know that the state reached with one VUV photon produces both HI^+ and I atoms. The ratio of HI^+ to I produced from this state is independent of the VUV intensity, and therefore applies equally to the spectra in Figs. 1 and 4. We also expect that the ratios of HI^+ to I produced from this level by one and three photons are approximately equal. Under the conditions of coherent control (that is, the conditions of Fig. 1) the concentrations of HI^+ produced by one and three photons are approximately equal. It follows that under the conditions of coherent control the concentrations of I produced by one and three photons are also approximately equal. We therefore conclude that the Rydberg structure, which dominates the one-photon spectrum in Fig. 4, is also present in the three-photon spectrum, although it is not readily visible at the poor signal-to-noise ratio of Fig. 1. It is still possible that under the conditions of coherent control there is also a contribution to the total I^+ signal generated at the two-photon level. Because the phase dependence of the controlled signal is tied to the Rydberg structure of HI, it is evident that the two-photon contribution is minor.
22. J. Berkowitz, C. H. Batson, G. L. Goodman, *Phys. Rev. A* **24**, 149 (1981); F. Robicheux and C. H. Greene, *ibid.* **46**, 3821 (1992).

23. We thank H. Lefebvre-Brion for many helpful discussions and the National Science Foundation for its support.

15 June 1995; accepted 24 July 1995

Radar Images of Asteroid 4179 Toutatis

Steven J. Ostro,* R. Scott Hudson, Raymond F. Jurgens,
Keith D. Rosema, Donald B. Campbell, Donald K. Yeomans,
John F. Chandler, Jon D. Giorgini, Ron Winkler, Randy Rose,
S. Denise Howard, Martin A. Slade, Phil Perillat, Irwin I. Shapiro

Delay-Doppler images of the Earth-crossing asteroid 4179 Toutatis achieve resolutions as fine as 125 nanoseconds (19 meters in range) and 8.3 millihertz (0.15 millimeter per second in radial velocity) and place hundreds to thousands of pixels on the asteroid, which appears to be several kilometers long, topographically bifurcated, and heavily cratered. The image sequence reveals Toutatis to be in an extremely slow, non–principal axis rotation state.

Optical investigations of Earth-orbit–crossing asteroids (ECAs) are limited by their small angular sizes (typically ≪1 arc sec), but radar measurements of the distribution of echo power in time delay and Doppler frequency can be used to synthesize images of these objects. Toutatis's approach to within 0.024 astronomical unit (AU) (9.4 lunar distances) on 8 December 1992 was an unprecedented opportunity for radar investigation of a small body. We present images that achieve areal resolutions ~100 times finer than previously obtained (*1*) for any ECA and reveal an object with startling characteristics.

The images were obtained with the Goldstone Radar in California daily from 2 to 18 December and at the Arecibo Observatory in Puerto Rico daily from 14 to 19 December (Table 1). We used binary-phase coded wave forms (*2*) that provided a time resolution Δt equal to the temporal extent of each code element, a range resolution equal to Δt times half the speed of light, and a frequency resolution

$$\Delta f = 1/(RP \times N_{\mathrm{COH}} \times L_{\mathrm{FFT}}) = 1/T_{\mathrm{COH}} \qquad (1)$$

where the code repetition period RP equals Δt times the number of elements in the code (255 for Goldstone, 8191 for Arecibo) and N_{COH} is the number of successive, RP-

S. J. Ostro, R. F. Jurgens, K. D. Rosema, D. K. Yeomans, J. D. Giorgini, R. Winkler, R. Rose, S. D. Howard, M. A. Slade, Jet Propulsion Laboratory, California Institute of Technology, Pasadena, CA 91109–8099, USA.
R. S. Hudson, School of Electrical Engineering and Computer Science, Washington State University, Pullman, WA 99164–2752, USA.
D. B. Campbell, National Astronomy and Ionosphere Center, Space Sciences Building, Cornell University, Ithaca, NY 14853–6801, USA.
J. F. Chandler and I. I. Shapiro, Center for Astrophysics, 60 Garden Street, Cambridge, MA 02138, USA.
P. Perillat, Arecibo Observatory, Box 995, Arecibo, Puerto Rico 00613, USA.

---

*To whom correspondence should be addressed at mail stop 300-233. E-mail: ostro@echo.jpl.nasa.gov